https://doi.org/10.3311/PPtr.22918

Periodica Polytechnica Transportation Engineering, 52(2), pp. 190–198, 2024

Friction and Wear of the Piston Ring – Cylinder Liner System with Artificially Aged Ultra-low Viscosity Engine Oils

András Lajos Nagy[1*]

[1] Department of Propulsion Technology, Audi Hungaria Faculty of Automotive Engineering, Széchenyi István University, Egyetem tér 1., H-9026 Győr, Hungary
[*] Corresponding author, e-mail: nagy.andras1@sze.hu

Received: 02 July 2023, Accepted: 29 October 2023, Published online: 09 January 2024

Abstract

This study aims to investigate the performance of artificially aged prototype engine oils through friction and wear experiments. Experiments were performed on a piston ring – cylinder liner model system with boundary conditions derived from real-life operating conditions. The experimental design implemented two prototype oils (SAE 0W-12 and 0W-16) in unaltered and artificially aged form. An additional fully formulated off-the-shelf engine oil (SAE 0W-20) was also aged and analyzed as reference. Oil samples were artificially aged in a custom rig, to simulate long-term in-engine use through thermal cycling at 180 °C. Fourier Transformed Infrared Spectroscopy of the lubricant samples highlighted a depletion of zinc dialkyl-ditiophosphate antiwear additives in all cases, which is comparable to a selected in-service oil. Oxidation was also measurable, albeit lower compared to the in-service sample. Averaged friction coefficients showed a ranking of aged 0W-12 < aged 0W-16 < unaltered 0W-12 < unaltered 0W-16. A decrease in surface roughness was experienced with aged oil samples, whereas unaltered 0W-16 oil produced an unexpected transition in the wear phenomenon and resulted in severe wear.

Keywords

artificial engine oil degradation, piston ring wear, cylinder liner wear, tribometry, wear analysis

1 Introduction

With a large variance in regional out-phasing roadmaps of internal combustion engine powertrains (Jin et al., 2021; News European Parliament, 2023; Muratori et al., 2023), synthetic alternative fuels and novel low-viscosity engine oil formulations could pose as viable bridge technologies with a positive impact on GHG emissions of conventional and hybrid drivetrain vehicles through climate neutral fueling and a reduction of mechanical losses.

The piston ring – cylinder liner subsystem alone contributes to 20–50% of mechanical losses of an ICE (Götze and Jaitner, 2022; Liao et al., 2012; Richardson, 2000), depending on the design and operating conditions. On a system level, this translates to around 7% of total losses (D'agostino and Senatore, 2006), which is caused by a limited number of components. In order to optimize friction losses in the ring-liner system, a number of factors must be considered. An optimal contact pressure distribution on the ring's surface is fundamental in achieving the desired combustion chamber sealing, oil consumption control, and heat transfer from piston to cylinder, while maintaining a low coefficient of friction (Morris et al., 2017). In addition to ring geometry and tension, engine oil viscosity (Harigaya et al., 2006) largely contributes to lubricant film thickness on the cylinder liner. A change in oil viscosity through oil dilution as a result of novel fuel formulations (Ljubas et al., 2010; Tilli et al., 2018), or the application of cutting-edge oils with reduced viscosity could lead to unknown circumstances, e.g., elevated wear (Sagawa et al., 2017).

This article aims to give a brief look into friction and wear of the piston ring – cylinder liner tribosystem of a 4-cylinder turbocharged gasoline direct injection (GDI) engine under lubrication with artificially altered pre-series production engine oils through friction and wear experiments performed on a tribometer.

1.1 Scientific overview

A number of articles have dealt with the topic of piston ring tribology and engine oil degradation and highlighted the complexity of the key governing phenomena regarding friction and wear in the system.

Cite this article as: Nagy, A. L. (2024) "Friction and Wear of the Piston Ring – Cylinder Liner System with Artificially Aged Ultra-low Viscosity Engine Oils", Periodica Polytechnica Transportation Engineering, 52(2), pp. 190–198. https://doi.org/10.3311/PPtr.22918

Lenauer et al. (2015) examined artificially aged Group I pre-formulated SAE 15W-40 engine oil (*A*), and Group III SAE 5W-30 engine oil (*C*) treated with ethanol combustion by-products. Gray cast iron cylinder liners and nitrided X90CrMoV18 steel piston rings were used for the experiments. Optimol SRV4 tribometer tests were performed under conditions derived from loads at the top dead center piston position. Results showed that the usage of aged lubricants resulted in lower steady-state wear rates and thinner tribofilms compared to the corresponding unaltered oils.

In a follow-up study, Spiller et al. (2017) investigated the durability of tribofilms formed on the contact surface of piston ring – cylinder liner parts. Fresh and artificially aged pre-formulated SAE 5W-30 engine oils and a PAO8 poly-alpha-olefin base oil were used for the experiments. When compared to the pre-formulated oils, the investigated PAO8 oil exhibited higher carbon content in the tribofilm, while Zn and S was not present on the surface. Furthermore, the artificial aging of the lubricants generated acidic species in the oil, leading to a carbon-rich tribofilm formation compared to fresh oil. The observed higher initial wear during the use of aged oils indicated that it takes more time to form an acidic tribofilm compared to fresh oils.

Obert et al. (2016) replicated the tribology of the piston ring – cylinder liner system based on in-engine conditions around the top dead center. Experiments were conducted on an Optimol SRV3 tribometer equipped with a self-developed rotating unit to establish the appropriate lubrication conditions. The oil supply was regulated using an HPLC pump. The lubricants used were pre-formulated engine oils with viscosities according to SAE 5W-30, 0W-30, and 0W-20 classes. Wear measurements were performed using confocal microscopy. In most cases, the coefficient of friction (COF) values remained around 0.15 regardless of the load case. An approximately linear decrease in the lubricant consumption coefficient (LCC) was observed with increasing temperature. Additionally, high temperature and very low oil supply rate resulted in a significant decrease in LCC.

Costa et al. (2021) assessed the structure of ZDDP tribofilms using synchrotron radiation-based X-ray absorption near edge structure spectroscopy and XPS measurements. Tribological tests were performed on an Optimol SRV4 tribometer under a normal load of 150 N, a stroke length of 5 mm, and a frequency of 10 Hz. In all experiments, a solution of ZDDP additive in PAO8 base oil was used. This lubricant was also examined with the addition of anhydrous and hydrous ethanol at a dilution level of 5 wt. %. The results showed that ethanol increased friction and surface damage. Furthermore, the presence of ethanol led to a decrease in the quantity of long-chain phosphates, resulting in reduced antiwear performance. Sulfides in the tribofilms were found to be richer in iron in the presence of ethanol, indicating an increase in wear.

Drawing upon the research results presented above, an experimental procedure involving artificial engine oil aging, viscometry, infrared spectroscopy, SRV tribometer experiments, surface topology measurements, scanning electron microscopy and energy dispersive X-Ray spectroscopy is applied to investigate friction, wear and tribofilm properties with a selection of ultra-low viscosity engine oils.

2 Materials and methods

The conducted experimental study is based on model investigations of the ring – liner system. The investigated tribosystem comprises of an atmospheric plasma spray coated steel cylinder liner surface, and a chromium coated piston ring. Cylinder liner segments were manufactured through electric discharge machining, in order to maintain a high accuracy (squareness, parallelism) of the mating surfaces of the sample with the test rig's sample stage to reduce misalignment. Piston ring segments were cut from production parts on a laboratory cutting machine, as in this case the cut surfaces are not used for mating and alignment. Friction and wear experiments were implemented on an Optimol SRV5 tribometer (Optimol Instruments Prüftechnik GmbH, Munich, Germany). A custom load case was developed to ensure quantifiable wear results and manageable test durations. Test parameters were based on an estimation of in-engine conditions near the top dead center position during combustion at an intermediary load level. The resulting oscillation frequency, nominal load, part temperature, and stroke are detailed in Table 1.

Tribometry results include measured load, stroke, and mean coefficient of friction results with a 1-second averaging time. The resulting worn surfaces were scanned on a Leica DCM3D confocal measuring microscope

Table 1 Boundary conditions and parameters for friction and wear testing

Parameter	Value
Run-in procedure	(ASTM International, 2021)
Part temperature	120 °C
Oil temperature	120 °C
Total test time	16 hours
Run-in time	8 hours
Test load	200 N
Frequency	20 Hz
Stroke	3 mm

(Leica Microsystems GmbH, Wetzlar, Germany) to assess surface topography. Cylinder liner surfaces were analyzed in two sampling areas (worn and new) at 100x magnification, resulting in a 75 × 75 µm² evaluation area with 0.166 µm lateral spacing. Piston rings were similarly evaluated inside and outside the wear scar, using 50x magnification, resulting in a 225 × 225 µm² evaluation area with 0.332 µm lateral spacing. Pre-processing of topography slides included levelling, filling non-measured points based on their neighborhood, and the decomposition of waviness and roughness through Gaussian filtering with L_c = 25 µm. Surface roughness parameters were calculated in a batch process for all measured samples using LeicaMap 6.2 (Digital Surf, Besançon, France). Selected samples were investigated with energy dispersive X-Ray spectroscopy (EDX) in a Zeiss EVO 10 scanning electron microscope (Carl Zeiss AG, Oberkochen, Germany) for traces of oil additives in the worn area.

2.1 Engine oil aging and analysis

An SAE 0W-12 and SAE 0W-16 prototype oil, and a fully formulated off-the-shelf SAE 0W-20 engine oil was selected for the purpose of this study. Detailed chemical composition data is not available for the oils; however, it is established, that all oils have a poly-alpha-olefin base and are enhanced with zinc dialkyl-ditiophosphate antiwear additive. The selected engine oils were subjected to artificial engine oil aging in a custom developed laboratory oil aging rig (Nagy, 2019; Nagy and Zsoldos, 2021). A 200 ml sample of each oil was aged for 96 hours in 12-hour long degradation phases at 180 °C, followed by 12-hour long polymerization phases at room temperature. Compressed air was routed through the samples at 1.1 bar pressure and a constant airflow of 1 l/min. A total of 4 engine oil samples were subjected to friction and wear experiments:

- unaltered reference samples REF 0W-12, and REF 0W-16,
- artificially aged oil samples AGE 0W-12, and 0W-16.

Key properties of the unaltered reference samples are summarized in Table 2.

Table 2 Oil sample names and measured kinematic viscosity values for unaltered reference samples

Oil sample	Kin. visc. 40 °C	Kin. visc. 100 °C
REF 0W-20	39.72 mm²/s	7.92 mm²/s
REF 0W-16	33.42 mm²/s	7.02 mm²/s
REF 0W-12	28.82 mm²/s	5.86 mm²/s

Kinematic viscosity of test oils was measured on a Stabinger SVM3001 viscosimeter (Anton Paar GmbH, Graz, Austria). Fourier Transformed Infrared Spectroscopy (FTIR) was performed on pre-aging and post-aging samples on a Bruker INVENIO-S infrared spectrometer (Bruker Corporation, Billerica, MA, USA) utilizing a diamond attenuated total reflectance (ATR) cell, to assess oxidation, and antiwear additive depletion. Quantified results are calculated based on spectral subtraction according to (ASTM International, 2018).

2.2 Design of experiments

A resolution III type screening (fractional factorial) experimental design with 3 factors at 2 levels was implemented in order to maximize information gained from the available experimental budget. Factors in the experiments were:

- *A*: engine oil condition, with reference oils being low level, and aged oils being high level;
- *B*: engine oil type, with 0W-12 being low level, and 0W-16 being high level;
- *C*: oil volume, with one drop (0.1 ml at the start of the experiment) being low level, and continuous (0.1 ml / hour administered through an external syringe pump) being high.

The factors and levels of the screening experiments are summarized in Table 3. Factor *C* is confounded with the two-factor interaction of factors *A* and *B*, where:

$$C = -A \times B.$$

Additional reference measurements were carried out with the SAE 0W-20 fully formulated engine oil. Each experiment was replicated three times to ensure consistent results and account for the noise in the system. The evaluated response for all measurements was averaged friction coefficient after run-in. Linear models were developed in R (R Core Team, online) and analyzed with the PID package (Dunn, online). Data preprocessing tasks – i.e., collection and handling of individual tribometry result files, as well as grouping, filtering, basic statistics calculations, and plotting – were conducted in Python (Van Rossum

Table 3 Standard order table of the implemented experimental design

Series	*A* (condition)	*B* (type)	$C = -A \times B$ (lubrication)
1	− (REF)	− (0W-12)	− (one drop)
2	+ (AGE)	+ (0W-16)	− (one drop)
3	− (REF)	+ (0W-16)	+ (continuous)
4	+ (AGE)	− (0W-12)	+ (continuous)

and Drake, online) using the Pandas (Zenodo, online) and Plotly (Plotly Technologies Inc., online) libraries.

3 Results and discussion

3.1 Oil condition after artificial aging

Table 4 provides an overview of the kinematic viscosity of artificially aged oil samples. An in-use SAE 0W-30 engine oil sample is also shown for context, which represents the change in oil condition in a vehicle with a 4-cylinder turbocharged GDI engine after 1,119 km exclusively urban vehicle use, with a 99th percentile of speed at 56 km/h – i.e., the vehicle nearly never exceeded this speed. Measurement results for this sample were obtained in a prior experiment (Agocs et al., 2021) with non-identical instrumentation. As anticipated, aged oil samples show an increase in kinematic viscosity measured at 40 °C compared to the unaltered oils, as a result of the polymerization due to cyclic thermal load during artificial aging. However, this increase is less prominent at 100 °C, which highlights, that viscosity modifier additives were not affected by the applied aging procedure. In contrast to the in-use sample, the samples aged for this study show viscosity values 7–28% lower at 40 °C, and 20–40% lower at 100 °C. This phenomenon can be attributed to fuel dilution in the in-use sample, as the presented artificial aging procedure does not account for fuel uptake during aging.

FTIR spectroscopy results are presented in Fig. 1 as difference spectra of the reference and aged oil samples.

Positive values correspond to species increasing in number, whereas negative values highlight a decrease, or depletion of certain components. Regions of interest for oxidation and phosphorous antiwear (AW) additive depletion (ZDDP depletion) are highlighted for further evaluation. Discarded regions – i.e., fingerprint region of the lubricants, single hydrogen bond region, C-C single bond region – are not shown in Fig. 1.

Table 5 offers a concise summary of oxidation and phosphorous AW additive depletion.

Table 4 Oil sample names and measured kinematic viscosity values for artificially aged oil samples

Oil sample	Kin. visc. 40 °C	Kin. visc. 100 °C
AGE 0W-20	42.58 mm^2/s	7.98 mm^2/s
AGE 0W-16	40.90 mm^2/s	7.80 mm^2/s
AGE 0W-12	33.41 mm^2/s	5.86 mm^2/s
In-use 0W-30^{+}	46 mm^2/s	10 mm^2/s

$^{+}$ Obtained in a prior experiment, shown here for reference, values computed using the respective spectrum of unaltered SAE 0W-30 oil, not used in tribometer experiments

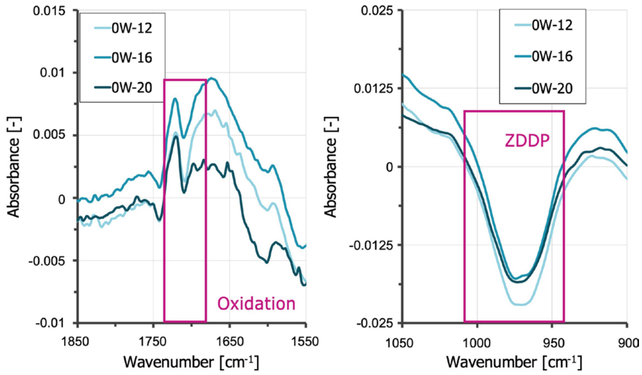

Fig. 1 Difference spectra of corresponding unaltered and aged engine oil samples. Regions of interest for oxidation (left) and ZDDP depletion (right) are highlighted

Table 5 Quantified oxidation and phosphorous AW additive (ZDDP) depletion

Oil sample	Oxidation [Abs / 0.1 mm]	ZDDP depletion [Abs / 0.1 mm]
AGE 0W-20	4.9×10^{-3}	-2.2×10^{-2}
AGE 0W-16	7.9×10^{-3}	-2.5×10^{-2}
AGE 0W-12	5.2×10^{-3}	-2.4×10^{-2}

Comparing the artificially aged samples reveals a nearly identical ZDDP depletion level, while oxidation values show a maximum difference of 38%, indicating the differences between prototype oils. The highest oxidation was experienced with 0W-16 oil. Further dissimilarities between artificially aged and in-use spectra in general stem from degradation phenomena that was not intended to be reproduced by the artificial aging process – e.g., nitration, that would appear as a minor peak between 1650 and 1610 cm^{-1}.

3.2 Friction and wear experiments

Table 6 shows the standard order table including measured responses for coefficient of friction (CoF) and the corresponding mean absolute deviation values (MAD).

Based on the response, a linear model is constructed, that has the form of:

$$y = I + b_A x_A + b_B x_B + b_C x_C . \quad (1)$$

Table 6 Standard order table with measured response average coefficient of friction, and the corresponding mean absolute deviation

Series	*A*	*B*	*C* (−*AB*)	CoF [-]	MAD
1	−	−	−	0.1762	0.0011
2	+	+	−	0.1793	0.0015
3	−	+	+	0.1880	0.0008
4	+	−	+	0.1705	0.0005

Coefficients b_A, b_B, and b_C, as well as the intercept I for linear model (Eq. (1)) are listed in Table 7.

Coefficient b_C is an order of magnitude smaller than b_A and b_B, thus has a very mild effect on the system. Comparing the coefficients with MAD values reveals, that b_C is not discernable from measurement noise, as the largest mean absolute deviation of a series (0.0015) is exactly two times as large as b_C. Coefficients b_A and b_B are at least two times larger than the noise of a measurement series, hence these can be considered significant. Thereby under the applied experimental conditions lubricant volume does not dictate the friction state in the system. As a result of this, the comparison of experiment series using one-drop and continuous lubrication is feasible and allows the assessment of aged and unaltered 0W-12 and 0W-16 oil samples.

A general assessment of measured CoF values reveals, that the experimental results are in accordance with the anticipated behavior, where runs with 0W-12 lubricants register lower coefficients of friction as runs with 0W-16 oil. Interestingly, aged engine oil samples show a decrease in CoF, which was unexpected, as viscometry has shown a significant drop after aging only for the 0W-16 sample. This phenomenon can be attributed to the friction states in the utilized reciprocating test setup. Fig. 2 illustrates the instantaneous CoF and ring speed plotted against displacement in a piston ring – cylinder liner tribosystem on the SRV5 tribometer, with 25 kHz data acquisition rate.

Friction increases at the ends of the stroke (at −1.5 and 1.5 mm in Fig. 2), as the piston ring comes to a halt and changes direction and decreases as the ring leaves the endpoints and moves towards the center of the stroke (at 0 mm in Fig. 2). Unfortunately, the test setup does not allow for a direct measurement of the oil film thickness. However, based on CoF and ring speed values it is reasonable to assume, that a boundary lubrication regime exists in the proximity of the endpoints, which gradually evolves into a mixed lubrication regime towards the center. These lubrication regimes – i.e., friction states – are more or less dominated by the tribofilm and are only partially governed by lubricant viscosity (Stribeck, 1902). Therefore, it is plausible to hypothesize, that the applied oil aging procedure resulted in the appearance of such reaction by-products, which facilitated the formation of a more robust tribofilm between contact surfaces.

Table 7 Intercept and coefficients for linear model (Eq. (1))

I	b_A	b_B	b_C
0.1785	−0.0036	0.00515	0.00075

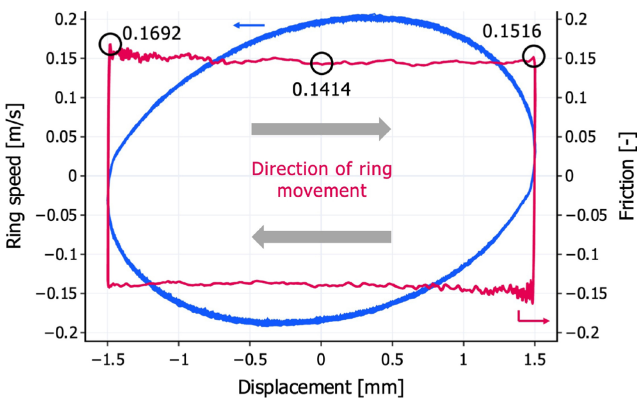

Fig. 2 Instantaneous coefficient of friction (red) and ring speed (blue) plotted against the displacement of the piston ring for 40 strokes, as measured on an SRV5 tribometer

Table 8 summarizes surface metrology results in terms of changes in arithmetic mean height S_a, reduced peak height S_{pk}, and dale void volume V_{vv}.

The average for each roughness parameter corresponding to individual measurements in a series was calculated, then the difference between values corresponding to worn and unworn regions was determined and summed up to represent the tribopairs in a series. The resulting compound surface roughness parameters are denoted as $\Delta\overline{S_a}$, $\Delta\overline{S_{pk}}$, $\Delta\overline{V_{vv}}$, and can be referred to as average differential arithmetic mean height, average differential reduced peak height, and average differential dale void volume, respectively.

In general, aged 0W-12, aged 0W-16 and unaltered 0W-12 oils show an anticipated ranking. Similarly to friction coefficients, the most prominent difference in surface roughness was established with the unaltered 0W-16 oil samples. Experiments with unaltered 0W-16 show an increase in all three investigated surface roughness parameters, which suggests severe wear. This phenomenon could be a result of insufficient tribofilm formation on the metallic surfaces during the experiment. To illustrate the extent and nature of wear with the outlier sample, Fig. 3 presents confocal microscopy slides of unworn (Fig. 3 (a) and (c)) and worn (Fig. 3 (b) (d)) surface configurations for selected cylinder liners corresponding to experiments with aged and unaltered 0W-16 oils. As depicted in the bottom

Table 8 Difference of measured surface roughness parameters (worn surface parameter minus unworn surface parameter)

Oil sample	$\Delta\overline{S_a}$ [μm]	$\Delta\overline{S_{pk}}$ [μm]	$\Delta\overline{V_{vv}}$ [μm³/μm²]
AGE 0W-12	−0.267	−0.305	−0.040
AGE 0W-16	−0.233	−0.253	−0.030
REF 0W-12	−0.172	−0.208	−0.018
REF 0W-16	0.644	0.619	0.102

right portion of Fig. 3, the original surface characteristics – i.e., spray coated kernel boundaries (Fig. 3 (a) / 1), honing marks (Fig. 3 (a) / 2), and surface porosity (Fig. 3 (a) / 3) – have completely disappeared, and new pits have formed (Fig. 3 (d) / 4) on the cylinder surface after friction and wear experiments with unaltered 0W-16 oil.

Taking a look at electron microscopy images (Fig. 4) further proves the existence of an alternative wear process for unaltered 0W-16 compared to its artificially aged variant.

With the latter the cylinder liner's surface retains the characteristics of its unworn state – i.e., visible honing marks (Fig. 4 (a) / 1) and surface pores (Fig. 4 (a) / 2) – with mild abrasive wear marks appearing on the surface (Fig. 4 (a) / 3). In comparison, neither the original surface configuration, nor signs of mild abrasive wear are visible on the liners surface after testing with the unaltered 0W-16 lubricant (Fig. 4 (b)).

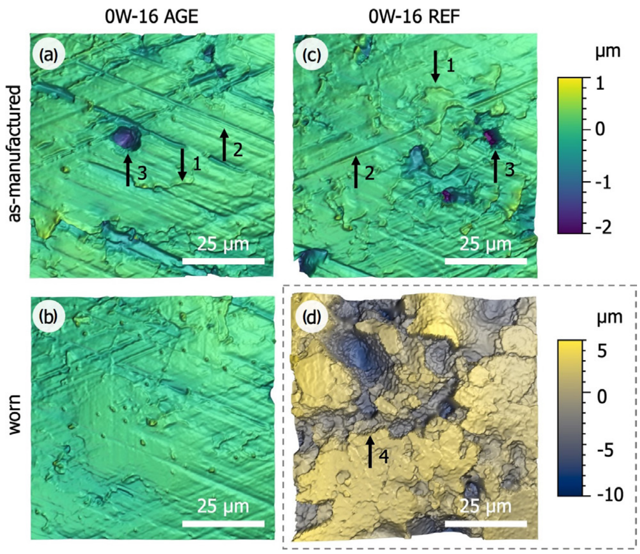

Fig. 3 Confocal microscopy slides of as-manufactured and worn surface configurations for selected cylinder liner samples of experiments with aged and unaltered 0W-16 oils. Numbers mark spray coated kernel boundaries (1), honing marks (2), naturally occurring pores (3) and severe wear (4); (a) liner surface before testing with aged 0W-16 oil; (b) liner surface after testing with aged 0W-16 oil; (c) liner surface before testing with fresh 0W-16 oil; (d) liner surface after testing with fresh 0W-16 oil

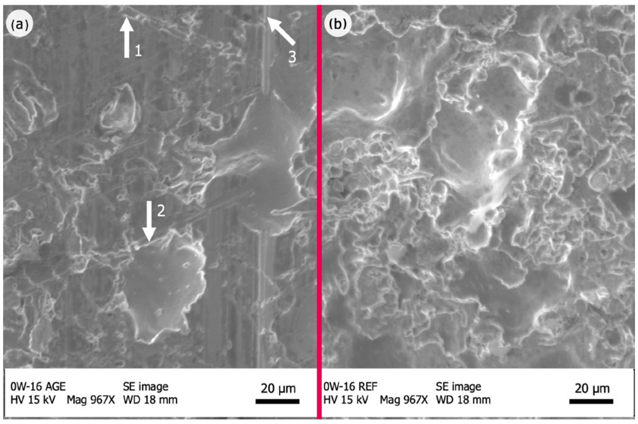

Fig. 4 Scanning electron microscopy slides of worn surface configurations for selected cylinder liners after experiments with aged (a) and unaltered (b) 0W-16 oils. Numbers mark honing marks (1), naturally occurring pores (2) and mild abrasive wear tracks (3)

The corresponding EDX spectra (Fig. 5) show elevated amounts of Na (detergent additive), P (antiwear additive), and S (extreme pressure additive) on the surface with the unaltered oil, which contradicts the assumption of no tribofilm formation as the cause of elevated wear. In both cases a strong presence of adhered Cr from the ring is reported, as well as C residue from the oils. Traces of Si (antifoaming additive) and Ca (detergent additive) are also visible on the spectra.

A detailed look at friction coefficient time series data corresponding to experiment series 3 with unaltered 0W-16 brings to light an abrupt transition from the expected operating condition to an elevated friction state, that signals a change in the dominant wear phenomenon. Fig. 6 depicts coefficient of friction values as a function of measurement time for the three repetitions of friction and wear measurements with unaltered 0W-16 engine oil.

Only a range of interest is presented, where the transition in friction and wear appears. Experiment 1 and 2 in series 3 exhibit anomalies in friction after the run-in phase, whereas the dominant wear phenomenon starts to transform in experiment 3 during the run-in phase, around 20,000 second (5.5 hours) into the experiment. This phenomenon is unlikely to stem from insufficient lubrication, as all experiments with unaltered 0W-16 oil were conducted with continuous lubrication.

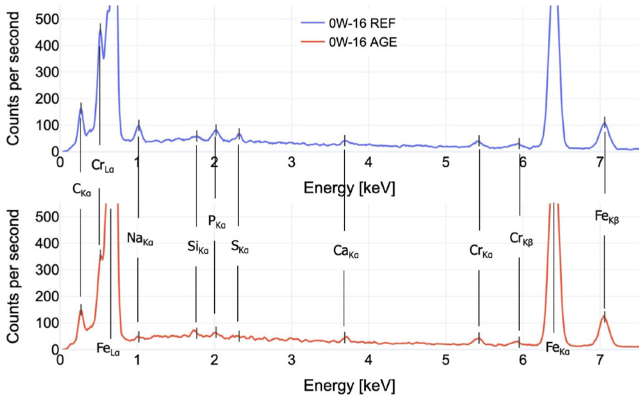

Fig. 5 Energy dispersive X-ray spectra of selected cylinder liner samples tested with aged and unaltered SAE 0W-16, showing element traces of the cylinder (Fe), piston ring (Cr), and common components in engine oils (C, Na, Si, P, S, Ca). Iron peaks are clipped for better visibility of comparably weaker peaks

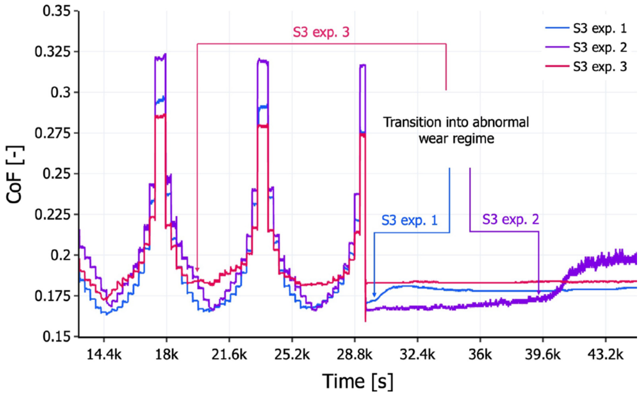

Fig. 6 Coefficient of friction time series data for repeated experiments with unaltered 0W-16 engine oil. Anomalies of CoF values in respect to the anticipated operating condition are highlighted for each experiment

As conditional high resolution data acquisition was not set up for this experiment, it is out of the scope of this study to further assess the unexpected behavior with unaltered 0W-16 oils. Additional investigation steps are necessary to fully understand what causes the above-mentioned transition and results in the collapse of the surface film and increase of wear rate.

4 Conclusion

This study aimed to investigate the effects of artificial aging on the performance of SAE 0W-12 and 0W-16 prototype engine oils in a tribological system using automotive piston ring and cylinder liner samples. The experiments involved testing both unaltered and aged oils, using a resolution III type screening experimental design on an SRV5 reciprocating tribometer. Oil condition was assessed through viscometry and FTIR spectrometry, whereas the contact pair was assessed using confocal microscopy, scanning electron microscopy, and energy dispersive X-ray spectroscopy.

The results of this study revealed the following insights regarding artificially aged engine oils, as well as the tribometric assessment of the piston ring – cylinder liner system:

- Artificial aging of 0W-12, 0W-16, and 0W-20 (as reference) engine oil samples resulted in a degradation of zinc dialkyl-ditiophosphate antiwear additive and measurable oxidation levels. 0W-16 oil showed the highest oxidation, which is presumably the results of disparities between used additive packages in the prototype oils.
- Viscometry revealed a measurable increase in the kinematic viscosity of the investigated 0W-16 oil at 100 °C, whereas other samples showed negligeable changes.
- Assessing results from the DoE showed, that using 0.1 ml lubricant at the start of the measurement, or a continuous 0.1 ml/hour lubrication setup has no clear effect on the coefficient of friction during the 16-hour experiment with the utilized tribosystem.
- In terms of coefficient of friction after run-in, the investigated oils showed an unusual ranking, with aged samples consistently reporting lower friction coefficients. This is believed to be a consequence of the experimental setup's reciprocating nature and slow overall speed, resulting in a tribofilm dominated friction state, as opposed to a lubricant viscosity dominated state at higher speed.
- Assessing the wear of the system through average differential roughness parameters $\Delta\overline{S_a}$, $\Delta\overline{S_{pk}}$, $\Delta\overline{V_{vv}}$ also revealed an anomaly in friction and wear. Experiments with the unaltered 0W-16 oil resulted in an increase of surface roughness, which was traced back to abnormal wear on the surface of the cylinder liner.
- The abnormality was assumed to be caused by a lack of tribofilm formation, which was rejected after SEM and EDX analysis of the surface, which showed trace elements typical to detergent, antiwear, and extreme pressure additives on the surface of a selected cylinder liner after testing with unaltered 0W-16.
- Analyzing coefficient of friction time series for runs with unaltered 0W-16 revealed an unexpected transition from normal operation conditions to an elevated friction state, which highlights an underlying transition into an abnormal wear phenomenon.

In summary, this research contributes to the understanding of tribological behavior in piston ring – cylinder liner tribosystems, and the influence of artificial engine oil aging, paving the way for improved lubricant selection and maintenance practices in automotive applications.

Acknowledgement

Supported by the ÚNKP-22-4-II-SZE-9 New National Excellence Program of the Ministry for Culture and Innovation from the source of the National Research, Development and Innovation Fund.

References

Agocs, A., Nagy, A. L., Tabakov, Z., Perger, J., Rohde-Brandenburger, J., Schandl, M., Besser, C., Dörr, N. (2021) "Comprehensive assessment of oil degradation patterns in petrol and diesel engines observed in a field test with passenger cars – Conventional oil analysis and fuel dilution", Tribology International, 161, 107079. https://doi.org/10.1016/j.triboint.2021.107079

ASTM International (2018) "ASTM E2412-10(2018) Standard Practice for Condition Monitoring of In-Service Lubricants by Trend Analysis Using Fourier Transform Infrared (FT-IR) Spectrometry", ASTM International, West Conshohocken, PA, USA. https://doi.org/10.1520/E2412-10R18

ASTM International (2021) "ASTM G181-21 Standard Test Method for Conducting Friction Tests of Piston Ring and Cylinder Liner Materials Under Lubricated Conditions", ASTM International, West Conshohocken, PA, USA. https://doi.org/10.1520/G0181-21

Costa, H. L., Evangelista, K. S., Cousseau, T., Acero, J. S. R., Kessler, F. (2021) "Use of XANES and XPS to investigate the effects of ethanol contamination on anti-wear ZDDP tribofilms", Tribology International, 159, 106997. https://doi.org/10.1016/j.triboint.2021.106997

D'agostino, V., Senatore, A. (2006) "Theoretical Analysis for Friction Losses Minimization in Piston Rings", In: Proceedings of the 5th International Conference on Tribology, Parma, Italy, p. 12. ISBN 8890233303

Dunn, K. G. "Process Improvement using Data", [online] Available at: https://learnche.org/pid [Accessed: 14 June 2023]

Götze, A., Jaitner, D. (2022) "Combined experimental and simulative approach for friction loss optimization of DLC coated piston rings", Automotive and Engine Technology, 7(3), pp. 283–293. https://doi.org/10.1007/s41104-022-00115-7

Harigaya, Y., Suzuki, M., Toda, F., Takiguchi, M. (2006) "Analysis of oil film thickness and heat transfer on a piston ring of a diesel engine: Effect of lubricant viscosity", Journal of Engineering for Gas Turbines and Power, 128(3), pp. 685–693. https://doi.org/10.1115/1.1924403

Jin, L., He, H., Cui, H., Lutsey, N., Wu, C., Chu, Y., Zhu, J., Xiong, Y., Liu, X. (2021) "Driving a Green Future", [pdf] The ICCT, Washington, DC, USA. Available at: https://theicct.org/wp-content/uploads/2021/06/China-green-future-ev-jan2021.pdf [Accessed: 28 May 2023]

Lenauer, C., Tomastik, C., Wopelka, T., Jech, M. (2015) "Piston ring wear and cylinder liner tribofilm in tribotests with lubricants artificially altered with ethanol combustion products", Tribology International, 82, pp. 415–422. https://doi.org/10.1016/j.triboint.2014.04.034

Liao, K., Chen, H., Tian, T. (2012) "The study of friction between piston ring and different cylinder liners using floating liner engine - Part 1", SAE International, Warrendale, PA, USA, 2012-01-1334. https://doi.org/10.4271/2012-01-1334

Ljubas, D., Krpan, H., Matanović, I. (2010) "Utjecaj razrjeđenja motornih ulja gorivom na njihovu viskoznost, plamište i gorište" (Influence of engine oils dilution by fuels on their viscosity, flash point and fire point), NAFTA, 61(2), pp. 73–79. [online] Available at: https://hrcak.srce.hr/49121 [Accessed: 28 May 2023] (in Czech)

Morris, N., Mohammadpour, M., Rahmani, R., Rahnejat, H. (2017) "Optimisation of the piston compression ring for improved energy efficiency of high performance race engines", Proceedings of the Institution of Mechanical Engineers, Part D: Journal of Automobile Engineering, 231(13), pp. 1806–1817. https://doi.org/10.1177/0954407016686249

Muratori, M., Kunz, T., Hula, A., Freedberg, M. (2023) "The U.S. National Blueprint for Transportation Decarbonization", [pdf] Department of Energy, Washington, DC, USA. Available at: https://www.energy.gov/sites/default/files/2023-01/the-us-national-blueprint-for-transportation-decarbonization.pdf [Accessed: 28 May 2023]

Nagy, A. L. (2019) "Development of an Artificial Aging Process for Automotive Lubricants", In: Spring Wind 2019, Debrecen, Hungary, pp. 102–108. ISBN 9786155586606

Nagy, A. L., Zsoldos, I. (2021) "Artificial Aging of Ultra-low Viscosity Lubricant Samples on a Programmable Oil Aging Rig", In: Vehicle and Automotive Engineering 3 (VAE 2020), Miskolc, Hungary, pp. 139–147. ISBN 978-981-15-9528-8 https://doi.org/10.1007/978-981-15-9529-5_12

News European Parliament (2023) "EU ban on the sale of new petrol and diesel cars from 2035 explained", News European Parliament, 30 June 2023. [online] Available at: https://www.europarl.europa.eu/news/en/headlines/economy/20221019STO44572/eu-ban-on-sale-of-new-petrol-and-diesel-cars-from-2035-explained [Accessed: 01 July 2023]

Obert, P., Müller, T., Füßer, H.-J., Bartel, D. (2016) "The influence of oil supply and cylinder liner temperature on friction, wear and scuffing behavior of piston ring cylinder liner contacts - A new model test", Tribology International, 94, pp. 306–314. https://doi.org/10.1016/j.triboint.2015.08.026

Plotly Technologies Inc. "Collaborative data science", [computer program] Available at: https://plot.ly [Accessed: 02 July 2023]

R Core Team "R: A Language and Environment for Statistical Computing", [computer program] Available at: https://www.r-project.org [Accessed: 02 July 2023]

Richardson, D. E. (2000) "Review of Power Cylinder Friction for Diesel Engines", Journal of Engineering for Gas Turbines and Power, 122(4), pp. 506–519. https://doi.org/10.1115/1.1290592

Sagawa, T., Nakano, S., Bito, Y., Koike, Y., Okuda, S., Suzuki, R. (2017) "Development of Low Viscosity API SN 0W-16 Fuel-Saving Engine Oil Considering Chain Wear Performance", SAE International Journal of Fuels and Lubricants, 10(2), pp. 469–477. https://doi.org/10.4271/2017-01-0881

Spiller, S., Lenauer, C., Wopelka, T., Jech, M. (2017) "Real time durability of tribofilms in the piston ring – cylinder liner contact", Tribology International, 113, pp. 92–100. https://doi.org/10.1016/j.triboint.2016.12.002

Stribeck, R. (1902) "Die wesentlichen Eigenschaften der Gleit- und Rollenlager" (The Essential Characteristics of Sliding and Roller Bearings), Zeitschrift des Vereines Deutscher Ingenieure, 46, pp. 1341–1348. (in German)

Tilli, A., Hulkkonen, T., Kaario, O., Larmi, M., Sarjovaara, T., Lehto, K. (2018) "Biofuel blend late post-injection effects on oil dilution and diesel oxidation catalyst performance", International Journal of Engine Research, 19(9), pp. 941–951. https://doi.org/10.1177/1468087417736466

Van Rossum, G., Drake, F. L. "Python 3", [computer program] Available at: https://www.python.org [Accessed: 02 July 2023]

Zenodo "pandas-dev/pandas: Pandas (v2.0.2)", [computer program] Available at: https://doi.org/10.5281/zenodo.7979740 [Accessed: 02 July 2023]